DOI: 10.1002/ejic.201000100

Near-Infrared Luminescent, Neutral, Cyclic Zn_2Ln_2 (Ln = Nd, Yb, and Er) Complexes from Asymmetric Salen-Type Schiff Base Ligands

Xing-Qiang Lü,*[a,b] Wei-Xu Feng,[a] Ya-Ni Hui,[a] Tao Wei,[a] Ji-Rong Song,[a] Shun-Sheng Zhao,[b] Wai-Yeung Wong,[b] Wai-Kwok Wong,*[b] and Richard A. Jones*[c]

Keywords: Zinc / Schiff bases / Lanthanides / Luminescence / Energy transfer

In the presence of excess pyridine (py), $Zn(OAc)_2{\cdot}2H_2O$ reacted with an equimolar amount of asymmetric salen-type Schiff base ligand, generated in situ from the condensation of 2,3-diaminophenol with *o*-vanillin or 5-bromo-3-methoxybenzaldehyde, to give the d-block "complex ligand" [Zn(HL^1)(py)] or [Zn(HL^2)(py)], respectively. Interaction of [Zn(HL^1)(py)] or [Zn(HL^2)(py)] with $Ln(NO_3)_3{\cdot}6H_2O$ in a 1:1 molar ratio gave the cyclic hetero-tetranuclear complexes $[Zn_2(L^1)_2(py)_2Ln_2(NO_3)_4(dmf)_2]{\cdot}3Et_2O$ (Ln = Nd, **1**; Yb, **2**; Er, **3**; and Gd, **4**) or $[Zn_2(L^2)_2Ln_2(NO_3)_4(dmf)_4]$ (Ln = Nd, **5**; Yb, **6**; Er, **7**; and Gd, **8**), respectively, in moderate yields. Photophysical studies of these cyclic Zn_2Ln_2 tetranuclear complexes showed that, upon photoexcitation in the 200–550 nm range corresponding to the intraligand $\pi\rightarrow\pi^*$ transition of the Schiff base, strong and characteristic NIR luminescence of Ln^{3+} ions with emissive lifetimes in the microsecond ranges were observed, whereas the ligand-centered singlet (^{1}LC) visible fluorescence was mostly quenched as a result of effective intramolecular energy transfer from the ^{1}LC excited state to the Ln^{3+} ions. In addition, the occupation of py groups at the axial position of Zn^{2+} ions and the involvement of heavy atoms seem to help to enhance the NIR luminescence to some extent.

Introduction

Ln^{3+} (Nd^{3+}, Yb^{3+} or Er^{3+}) complexes, with long-lived and characteristic linelike near-infrared (NIR) emission bands, have attracted much attention due to their potential applications in fluoroimmunoassay,[1] materials for optical telecommunication,[2] or organic light-emitting diodes (OLEDs).[3] However, for these lanthanide ions, because of the parity-forbidden nature of f–f transitions,[4] the absorption coefficients are normally very low ($\varepsilon \approx 1$–$10\ M^{-1}cm^{-1}$). To enhance their emissions, chromophores are often employed to transfer the absorbed energy efficiently to the lanthanide ions (the "antenna" effect). Though many cyclic[5] and acyclic[6] aromatic ligands with fully allowed $\pi\rightarrow\pi^*$ transitions in the UV region are designed for overcoming the low absorbance of these Ln^{3+} ions, it becomes more difficult to find ligand-centered chromophores absorbing at wavelengths longer than those in the UV region. The best source of chromophores, which absorb strongly in the visible region, is the d-block metal complexes[7] (i.e. Cr^{3+},[8] Co^{3+},[9] Zn^{2+},[10] Ru^{2+},[11] Pd^{2+},[12] Pt^{2+},[13] Ir^{3+},[14] Au^{+},[15] Ag^{+},[16] Cd^{2+},[17] Re^{+}, or Os^{2+}[18]) that display absorption bands at almost any desired wavelength and different excited states (^{1}LC, ^{3}LC, ^{3}MLCT, or ^{3}LMCT, where LC = ligand-centered, MLCT = metal-to-ligand charge transfer, LMCT = ligand-to-metal charge transfer) and have been demonstrated to effectively transfer energy to the Ln^{3+} ions indirectly.

Our past research work[19] has focused on the use of strongly fluorescent Zn–Schiff base complexes[20] as antennae or sensitizers for NIR luminescence of Ln^{3+} ions. We show that the selection of C_2 symmetric salen-type Schiff base ligands with inner N_2O_2 coordination sites and/or outer O_2O_2 portions is apt to bind with both 3d Zn^{2+} and 4f Ln^{3+} ions, and multinuclear heterometallic complexes have been constructed from functional bridges with OH,[21] anionic,[22] or pyridyl groups[23] and multidentate spacers with bipyridyl[24] or bicarboxylate ligands,[25] leading to enhanced NIR luminescence properties. To the best of our knowledge, there has been no report on the photophysical properties of the 3d–4f heterometallic complexes of asymmetric salen-type Schiff base ligands, though a few reports[26] have shown that asymmetric amide-imine Schiff base ligands can yield 3d–4f polynuclear molecules as novel single-molecule magnets (SMM) with large magnetic moments and magnetic anisotropy. If an OH group was incorporated into the linker of the salen-type Schiff base ligands, a new type of asymmetric salen-type Schiff base ligands

[a] Shaanxi Key Laboratory of Degradable Medical Material, Shaanxi Key Laboratory of Physico-inorganic Chemistry, Northwest University,
Xi'an 710069, Shaanxi, P. R. China
E-mail: lvxq@nwu.edu.cn
[b] Department of Chemistry and Centre for Advanced Luminescence Materials, Hong Kong Baptist University, Waterloo Road, Kowloon Tong, Hong Kong, P. R. China
E-mail: wkwong@hkbu.edu.hk
[c] Department of Chemistry and Biochemistry, The University of Texas at Austin,
1 University Station A5300, Austin, TX 78712-0165, USA
E-mail: rajones@mail.utexas.edu

with an inner N_2O_2 coordination site, an outer O_2O_2 cavity, and a coordinating oxygen atom from the OH group would be obtained. Use of this type of ligand could then give rise to new 3d–4f complexes of higher nuclearity through electron donation from the OH group. Another variation is the coordination of pyridine (py) at the axial position of 3d Zn^{2+} ions, which could serve to further increase the congestion around the coordination sphere of 4f Ln^{3+} ions, effectively decreasing luminescence quenching from OH-containing solvents around the lanthanide ions.[27] Furthermore, the presence of heavy Br atoms on the asymmetric Schiff base ligand could help to increase the quantum yield for triplet state formation and enhance the NIR sensitization of the Ln^{3+} ion.[28] Herein, we report the syntheses and structures of two series of cyclic hetero-tetranuclear complexes: $[Zn_2(L^1)_2(py)_2Ln_2(NO_3)_4(dmf)_2]\cdot 3Et_2O$ (Ln = Nd, **1**; Yb, **2**; Er, **3**; and Gd, **4**) and $[Zn_2(L^2)_2Ln_2(NO_3)_4(dmf)_4]$ (Ln = Nd, **5**; Yb, **6**; Er, **7**; and Gd, **8**). Their photophysical properties and sensitization of NIR luminescence of Ln^{3+} ions are also discussed.

Results and Discussion

Synthesis and Characterization

The reaction of $Zn(OAc)_2\cdot 2H_2O$ with an equimolar amount of the asymmetric salen-type Schiff base ligand, generated in situ from the condensation of 2,3-diaminophenol with *o*-vanillin or 5-bromo-3-methoxybenzaldehyde, in the presence of excess py in absolute EtOH, afforded the respective d-block "complex ligand" precursor $[Zn(HL^1)(py)]$ or $[Zn(HL^2)(py)]$ in 60% yield. Further reaction of the precursor with $Ln(NO_3)_3\cdot 6H_2O$ in a 1:1 molar ratio gave the cyclic hetero-tetranuclear complexes $[Zn_2(L^1)_2(py)_2Ln_2(NO_3)_4(dmf)_2]\cdot 3Et_2O$ (Ln = Nd, **1**; Yb, **2**; Er, **3**; and Gd, **4**) or $[Zn_2(L^2)_2Ln_2(NO_3)_4(dmf)_4]$ (Ln = Nd, **5**; Yb, **6**; Er, **7**; and Gd, **8**) (Scheme 1), which were isolated as microcrystalline solids upon slow diffusion of Et_2O into a solution of the respective compound in EtOH/dmf. In each series (**1**–**4** or **5**–**8**), it was shown that the coordination number for Ln (Nd, Yb, Er, and Gd) is the same, and all of them are isostructural and have the same ligand composition. This can be confirmed by the X-ray powder diffraction measurements of the bulk, as-prepared products **2**–**3** or **6**–**7**, which have diffraction patterns comparable with the simulated pattern from the single-crystal data (for **1** or **5**, respectively).

Compounds **1**–**8** are insoluble in water but more soluble in common organic solvents. These complexes were characterized by elemental analysis and FTIR spectroscopy. The solid-state structures of compounds **1** and **5** were ascertained by X-ray crystallography; pertinent bonding parameters are given in Table 1. For complex **1**, as shown in Figure 1, the phenoxo and methoxy oxygen atoms of the Zn^{2+} precursor $[Zn(HL^1)(py)]$ coordinate to one Nd^{3+} ion, and as expected, the oxygen atom from the OH group of the asymmetric Schiff base ligand on the opposite side coordinates to another Nd^{3+} ion, resulting in an alternate cyclic array of the Zn and Nd metal ions. Each Zn^{2+} ion has a five-coordinate environment and adopts a distorted square-pyramidal geometry composed of the inner N_2O_2 core from the Schiff base $(L^1)^{3-}$ ligand as the basal plane and one N atom from the coordinated py at the apical position, while the Nd^{3+} ions are in the outer O_2O_2 sites. The two ions are doubly bridged to one another through the two phenoxo O atoms of the Schiff base $(L^1)^{3-}$ ligand with a Zn···Nd separation of 3.644(2) Å. The Nd^{3+} ions are ten-coordinate. In addition to the two bridging phenoxo O atoms, their coordination environments are completed by eight other O atoms: four from two bidentate NO_3^- anions, two from OMe groups, one from the deprotonated OH group of the Schiff base $(L^1)^{3-}$ ligand, and one from the coordinated dmf solvate. The Nd–O bond lengths, depending on the nature of the oxygen atoms, vary from 2.329(4) to 2.735(4) Å, the bond length from the hydroxy oxygen atom being the shortest. The separation between the Zn^{2+} and Nd^{3+} ions bound

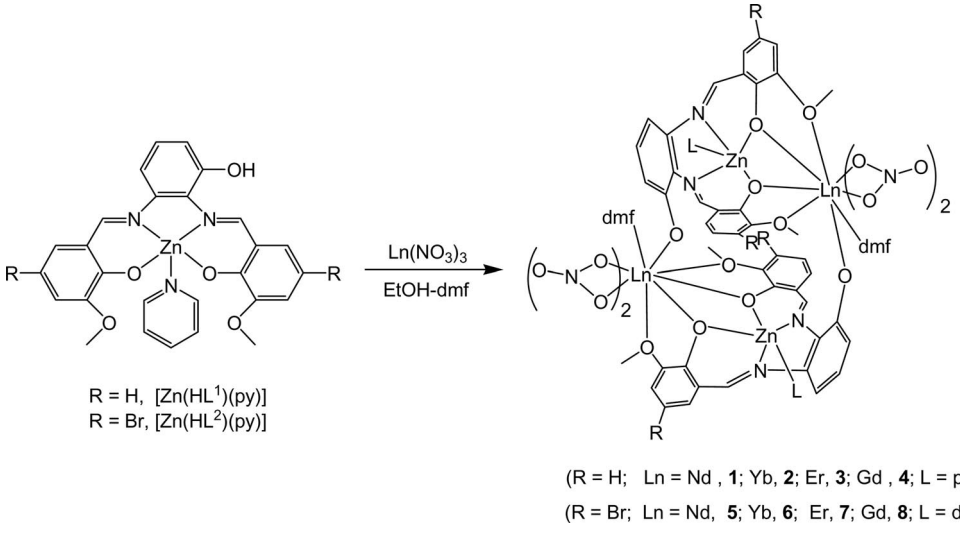

Scheme 1. Controlled design of cyclic tetranuclear heterometallic Zn_2Ln_2 complexes.

to each other through the oxygen atom from the deprotonated OH groups of the Schiff base $(L^1)^{3-}$ ligands is equal to 6.791(2) Å. The Et_2O molecules are solvents of crystallization; they are not bound to the framework and exhibit no observable interaction with the host structure. It is worth noting that the formation of cyclic tetranuclear complex **1** is incomparable to that of binuclear ZnLn complexes[19] of the C_2 symmetric Schiff base ligands without the involvement of the OH group, but is quite similar to that of the reported Cu_2Ln_2 complexes[26] from asymmetric amide-imine Schiff base ligands despite the lack of coordination of py groups at the apical position of the d-block metal ion.

Table 1. Interatomic distances (Å) and bond angles (°) with esds for **1** and **5**.

1		**5**	
Zn1–N1	2.067(4)	Zn1–N1	2.046(5)
Zn1–N2	2.020(5)	Zn1–N2	2.003(6)
Zn1–N3	2.063(4)	Zn1–O2	1.986(4)
Zn1–O2	1.993(4)	Zn1–O3	1.995(4)
Zn1–O3	2.011(3)	Zn1–O12	2.009(4)
Nd1–O1	2.700(3)	Nd1–O1	2.781(5)
Nd1–O2	2.424(3)	Nd1–O2	2.454(4)
Nd1–O3	2.485(4)	Nd1–O3	2.467(5)
Nd1–O4	2.735(4)	Nd1–O4	2.722(5)
Nd2–O5[a]	2.329(4)	Nd2–O5	2.621(5)
Nd1–O6	2.603(4)	Nd1–O7	2.542(5)
Nd1–O8	2.591(3)	Nd1–O8	2.594(5)
Nd1–O9	2.562(4)	Nd1–O10	2.589(5)
Nd1–O11	2.672(4)	Nd1–O11	2.315(4)
Nd1–O12	2.489(3)	Nd1–O13	2.477(5)
N1–Zn1–N2	80.90(17)	N1–Zn1–N2	81.0(2)
N1–Zn1–N3	102.07(17)	N1–Zn1–O2	92.0(2)
N1–Zn1–O2	89.95(16)	N1–Zn1–O3	147.23(17)
N1–Zn1–O3	145.25(15)	N1–Zn1–O12	103.42(19)
O1–Nd1–O4	145.14(11)	O1–Nd1–O4	142.14(13)
O1–Nd1–O5[a]	75.65(11)	O1–Nd1–O11	77.22(15)
O1–Nd1–O12	146.15(11)	O2–Nd1–O3	63.01(15)
O2–Nd1–O3	62.44(12)	O5–Nd1–O7	49.44(17)
O6–Nd1–O8	48.75(13)	O8–Nd1–O10	47.62(18)
O9–Nd1–O11	48.93(12)	O11–Nd1–O13	72.22(16)

[a] $-x + 1, -y + 2, -z + 1$.

The presence of heavy Br atoms in the precursor [Zn(HL^2)(py)] did not lead to a significant change in the host structure of cyclic tetranuclear Zn_2Nd_2 complex **5**, but slightly changed the coordination environments of the Zn^{2+} ions (Figure 2). In complex **5**, each Zn^{2+} ion also has a five-coordinate environment and adopts a distorted square-pyramidal geometry composed of the inner N_2O_2 core from the Schiff base $(L^2)^{3-}$ ligand as the basal plane, with an O atom from one coordinated dmf solvate at the apical position in place of the N atom from the py group of the d-block [Zn(HL^2)(py)] precursor. While the actual stepwise formation of the two complexes (**1** and **5**) from a similar pyridine-containing precursor [Zn(HL^1)(py)] or [Zn(HL^2)-(py)] is yet to be studied, it is worth noting that the presence of heavy Br atoms did not lead to a change in the coordination environment of Nd^{3+} ions in the same self-assembled system, despite the slight difference between the crystal parameters of **1** and **5**.

Compounds **1**–**8** retained their tetranuclear structures in CH_3CN solution. This was supported by their ESI-MS spectra, which displayed a parent peak at an *m*/*z* value corresponding to the $[M - NO_3]^+$ fragment. For instance, **1**–**4** exhibited the $[Zn_2(L^1)_2(py)_2Ln_2(NO_3)_3(dmf)_2]^+$ peak at *m*/*z* 1686.41 (**1**), 1744.01 (**2**), 1732.45 (**3**), and 1712.43 (**4**); whereas **5**–**8** exhibited the $[Zn_2(L^2)_2Ln_2(NO_3)_3(dmf)_4]^+$ peak at 1992.72 (**5**), 2049.77 (**6**), 2038.76 (**7**), and 2018.74 (**8**). In fact, we have previously demonstrated that related dinuclear complexes $[Zn(\mu\text{-}L)Ln(NO_3)_3]$[19b–19d] and tetranuclear complexes $[Zn_2(\mu\text{-}L)_2Ln_2(4,4'\text{-bipy})(NO_3)_6]$[24] (L =

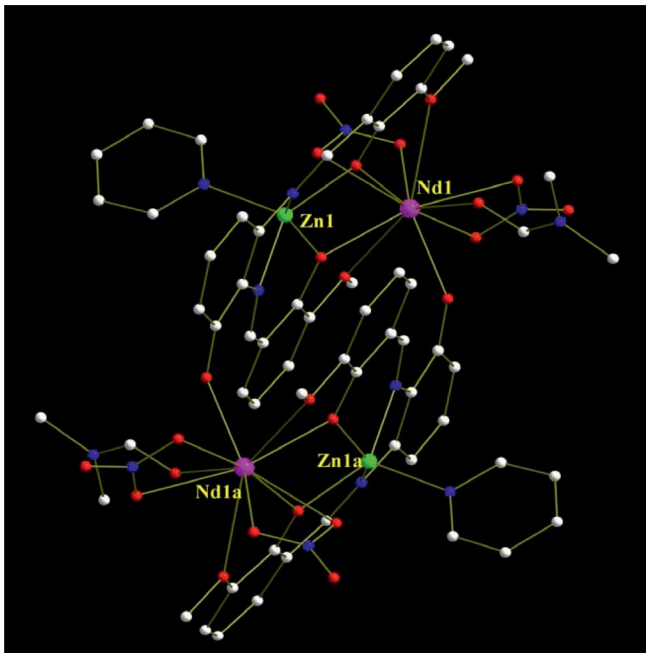

Figure 1. Perspective drawing of compound **1**; H atoms and solvates are omitted for clarity.

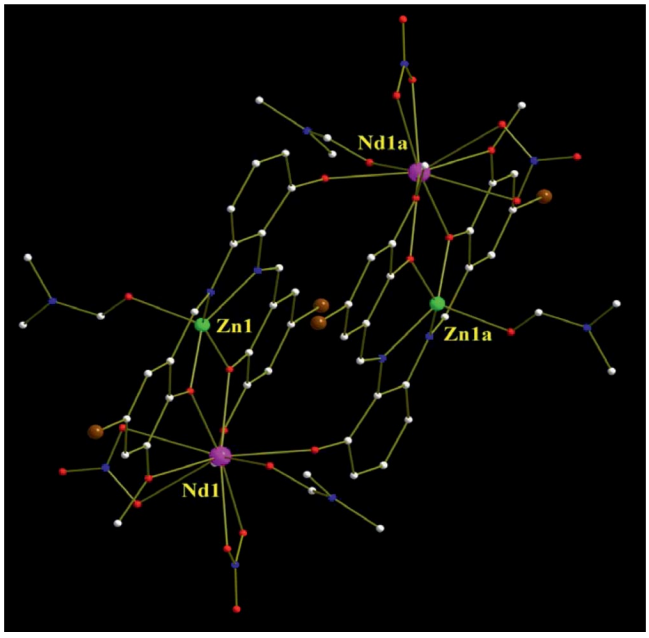

Figure 2. Perspective drawing of compound **5**; H atoms are omitted for clarity.

dianionic Schiff base ligand) existed as nonelectrolytes in CH_3CN and retained their solid-state structures in CH_3CN solution.

Photophysical Properties

The photophysical properties of [Zn(HL^1)(py)] and complexes **1**–**4** were examined in dilute CH_3CN solution at room temperature. Selected data are summarized in Table 2 and Figures 3, 4, and 5. As shown in Figure 3, complexes **1**–**4** display similar ligand-centered solution absorption spectra (250–255 and 322–329 nm) in the UV/Vis region. They are similar but blueshifted by 11–30 nm as compared to the absorption spectrum of the precursor [Zn(HL^1)(py)] (222, 266, and 352 nm). The absorptions of the tetranuclear complexes are stronger than that of the precursor at the same concentration. This is due to the presence of two chromophores for each tetranuclear complex and is in agreement with the solution behavior of discrete cyclic Zn_2Ln_2 arrays. For complexes **1**–**3**, weak visible emission bands (λ_{em} = 522 nm, τ = 2.10 ns for **1**; λ_{em} = 520 nm, τ = 2.86 ns for **2**; λ_{em} = 525 nm, τ = 1.75 ns for **3**) with low quantum yields ($\Phi_{em} < 10^{-5}$) in dilute CH_3CN solution at room temperature are observed, and they originate from the intraligand $\pi\rightarrow\pi^*$ transitions of the Schiff base ligand. In addition to the weak visible emission, photoexcitation of the antennae (λ_{ex} = 356 nm for **1**; λ_{ex} = 396 nm for **2**; λ_{ex} = 408 nm for **3**) gives rise to the characteristic emissions of the Nd^{3+} ($^4F_{3/2}\rightarrow{}^4I_{j/2}$, j = 9, 11, 13), Yb^{3+} ($^2F_{5/2}\rightarrow{}^2F_{7/2}$), and Er^{3+} ions ($^4I_{13/2}\rightarrow{}^4I_{15/2}$), respectively, in the NIR region (Figure 4). For **1**, the emissions at 883, 1068, and 1346 nm can be assigned to the $^4F_{3/2}\rightarrow{}^4I_{9/2}$, $^4F_{3/2}\rightarrow{}^4I_{11/2}$, and $^4F_{3/2}\rightarrow{}^4I_{13/2}$ transitions of the Nd^{3+} ion; and for **2** and **3**, the emissions centered at 975 and 1439 nm can be assigned to the $^2F_{5/2}\rightarrow{}^2F_{7/2}$ and $^4I_{13/2}\rightarrow{}^4I_{15/2}$ transitions of Yb^{3+} and Er^{3+} ions, respectively. The excitation spectra of complexes **1**–**3**, monitored at the respective NIR emission peak (1068 nm for **1**; 975 nm for **2**; 1439 nm for **3**) are similar to those monitored at the respective weak visible emission peak, clearly indicating that both visible and NIR emissions arise from the same intraligand $\pi\rightarrow\pi^*$ transitions of the Schiff base ligand, which suggests that the energy transfer from the antenna to these Ln^{3+} ions takes place efficiently.[29] For **1** and **2**, the respective NIR luminescence decay curves obtained from time-resolved luminescence experiments can be fitted monoexponentially with a time constant in the order of microseconds (λ_{em} = 883 nm, τ = 2.44 μs for **1**; λ_{em} = 975 nm, τ = 14.90 μs for **2**). The intrinsic quantum yield of Ln^{3+} emission (Φ_{Ln}) may be estimated by $\Phi_{Ln} = \tau_{obs}/\tau_0$, where τ_{obs} is the observed emission lifetime and τ_0 is the "neutral lifetime", 0.25 and 2.0 ms for

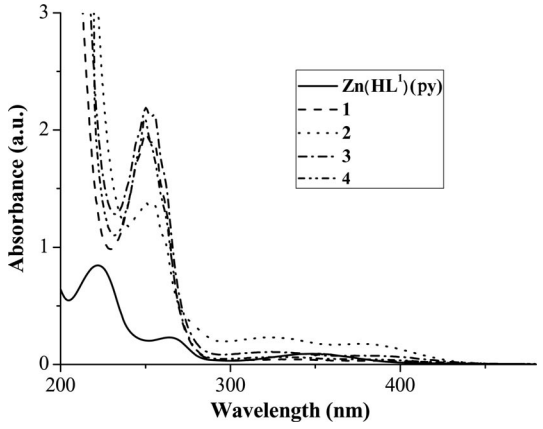

Figure 3. UV/Vis spectra of [Zn(HL^1)(py)] and complexes **1**–**4** in CH_3CN solution (1×10^{-5} M) at room temperature.

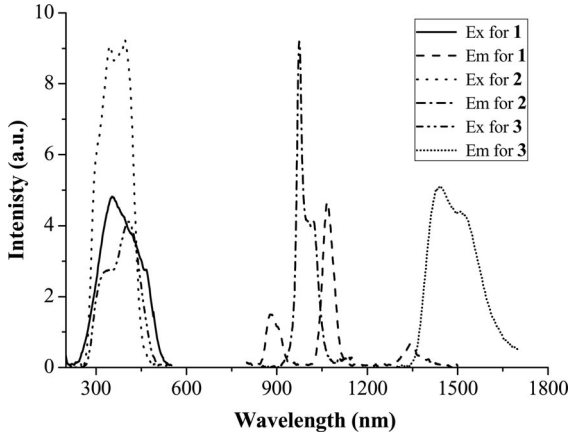

Figure 4. NIR emission and excitation spectra of complexes **1**–**3** in CH_3CN solution (1×10^{-5} M) at room temperature.

Table 2. Photophysical properties of [Zn(HL^1)(py)], [Zn(HL^2)(py)], and complexes **1**–**8** in CH_3CN solution (1×10^{-5} M) at room temperature or 77 K.

Compound	Absorption λ_{ab} (nm) [logε (dm^{3}mol^{-1}cm^{-1})]	Excitation λ_{ex} (nm)	Emission λ_{em} (nm) [τ, $\Phi\times10^3$]
[Zn(HL^1)(py)]	222 [0.85], 266 [0.23], 352 [0.09]	318, 400	524 [s, 2.52 ns, 17.92]
1	250 [1.97], 255 [1.90], 334 [0.04]	356, 416	522 [w, 2.10 ns, $<10^{-2}$], 883 [2.44 μs], 1068, 1346
2	249 [1.39], 254 [1.35], 322 [0.23]	346, 396	520 [w, 2.86 ns, $<10^{-2}$], 975 [14.90 μs]
3	250 [2.19], 254 [2.12], 324 [0.11]	338, 408	525 [w, 1.75 ns, $<10^{-2}$], 1439
4	250 [2.09], 329 [0.06]	315, 426	544 [s, 3.49 ns, 0.75], 532 [s, 5.41 ns, 77 K]
[Zn(HL^2)(py)]	214 [0.24], 327 [0.06], 412 [0.05]	327, 415	533 [s, 1.74 ns, 38.64]
5	319 [0.11], 389 [0.07]	322, 443	532 [w, 2.25 ns, $<10^{-2}$], 878 [1.17 μs], 1067, 1344
6	324 [0.09], 389 [0.07]	321, 440	535 [w, 2.10 ns, $<10^{-2}$], 974 [6.97 μs]
7	318 [0.13], 401 [0.08]	335, 448	534 [w, 1.44 ns, $<10^{-2}$], 1437
8	330 [0.06], 385 [0.04]	318, 438	538 [s, 2.99 ns, $<10^{-2}$], 532 [s, 5.41 ns, 2.6×10^{-2}, 77 K]

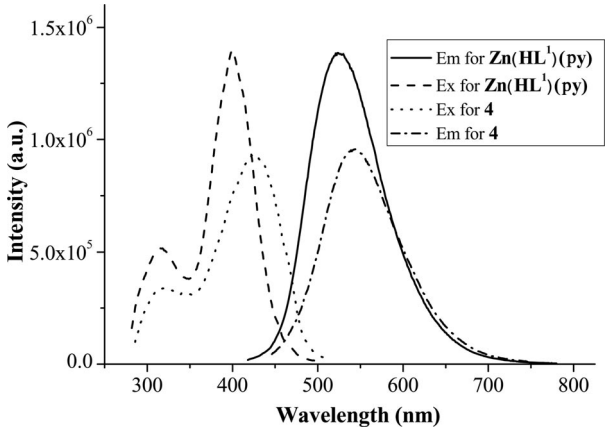

Figure 5. Visible emission and excitation spectra of [Zn(HL^1)(py)] and complex **4** in CH_3CN solution (1×10^{-5} M) at room temperature.

Nd^{3+} and Yb^{3+} ions, respectively.[30] The estimated Φ_{Ln} is 0.98 and 0.75% for **1** and **2**, respectively. This indicates that a unique and consistent coordination environment around the lanthanide ions is present despite the formation of the cyclic tetranuclear Zn_2Ln_2 structure.[31] The energy transfer efficiency of Nd^{3+} complex **1** is slightly better than that of Yb^{3+} complex **2**, which could be attributed to the wealth of accepting levels for the Nd^{3+} ion (versus only one for the Yb^{3+} ion).[32] Because of instrumental limitations, we were unable to determine τ_{obs} for the Er^{3+} ion and thus could not estimate Φ_{Ln} for the Er^{3+} ion, though strong NIR emission of the Er^{3+} ion was observed for complex **3**. The [Zn(HL^1)(py)] precursor does not exhibit any NIR luminescence under the same conditions. It merely displays the typical strong fluorescence (λ_{em} = 524 nm, τ = 2.52 ns, Φ_{em} = 17.92×10^{-3}) of the Schiff base ligand in the visible region (Figure 5).[20]

As a reference compound, Zn_2Gd_2 complex **4** allows the study of the antenna luminescence in the absence of energy transfer, because the Gd^{3+} ion has no energy levels below 32,000 cm^{-1}, and therefore cannot accept any energy from the excited state of the antenna (π*).[33] In dilute anhydrous CH_3CN solution (1×10^{-5} M), as shown in Table 2 and Figure 5, Zn_2Gd_2 complex **4** displays an emission centered at 544 and 532 nm at room temperature (r.t.) and 77 K, respectively. Time-resolved spectra showed that emission at both r.t. and 77 K corresponded to the ligand-centered singlet (^{1}LC) fluorescence with lifetimes of 3.49 and 5.41 ns, respectively. Ligand-centered triplet (^{3}LC) phosphorescence was not observed even at 77 K. These results indicate that the lowest triplet (T_1) state of the Schiff base ligand is nonemissive and probably decays by vibrational relaxation, and the sensitization of the NIR luminescence results from the ^{1}LC but not the ^{3}LC excited state of the ligand. Similar observations have been reported for related compounds.[19c] If the antenna luminescence lifetime of Zn_2Gd_2 complex **4** is to represent the populated excited-state lifetime in the absence of energy transfer, the energy transfer rate (k_{ET}) in the Zn_2Ln_2 complexes can thus be calculated from $k_{ET} = 1/\tau_{ZnLn} - 1/\tau_{ZnGd}$, where τ is the luminescence lifetime.[34] The calculated energy transfer rate for Zn_2Nd_2 (**1**, 1.9×10^8 s^{-1}) is higher than that for Zn_2Yb_2 (**2**, 0.6×10^8 s^{-1}) and lower than that for Zn_2Er_2 (**3**, 2.9×10^8 s^{-1}), which may result from the difference of the so-called spectral overlap of the antenna and the Ln^{3+} ions.[35] In spite of not having enough information on the NIR luminescence of **3**, we observed the strong NIR emission of the Er^{3+} ion unambiguously. This is different from the result of the reported symmetric phenylene-bridged Schiff base ZnEr complex,[19c] [Zn(L^3)Er(NO$_3$)$_3$(EtOH)] (H_2L^3 = *N*,*N*′-bis(3-methoxysalicylidene)phenylene-1,2-diamine), in which the NIR emission of the Er^{3+} ion was too weak to be observed. The reason could be due to the molecular design of the asymmetric salen-type Schiff base ligands. On formation of the cyclic Zn_2Er_2 molecule in **3**, the donating (antenna) levels match well with the receiving (Er^{3+} ion) levels.[36] In addition, the presence of py groups in axial positions of the 3d Zn^{2+} ions increases the steric congestion around the 4f Ln^{3+} ions and helps to decrease luminescence quenching from OH-containing solvents despite the existence of C–H vibrational oscillators of the coordinated dmf molecules.[27]

The presence of electron-withdrawing heavy Br atoms in the Schiff base ligand caused a redshift of the absorption (λ = 327, 415 nm) and emission (λ_{em} = 544 nm, Φ_{em} = 38.64×10^{-3}) spectra of [Zn(HL^2)(py)] relative to those of [Zn(HL^1)(py)]. As shown in Table 3 and Figures 6, 7, and 8, the partial quenching of the chromophore-based visible luminescence and the characteristic NIR emissions for complexes **5**–**7** are very similar to those of the Nd^{3+}(**1**), Yb^{3+}(**2**), and Er^{3+}(**3**) complexes, respectively. By using the antenna luminescence lifetime of Zn_2Gd_2 (**8**) as a reference for the excited-state lifetime in the absence of energy transfer, the calculated energy transfer rate for Zn_2Er_2 (**7**, 3.3×10^8 s^{-1}) is faster than those for Zn_2Nd_2 (**5**, 1.1×10^8 s^{-1}) and Zn_2Yb_2 (**6**, 1.4×10^8 s^{-1}). We were interested in comparing the photophysical properties between the two series of NIR luminescent complexes. For complexes **5**–**6**, from time-resolved luminescence experiments, the respective luminescence decay curve can also be fitted monoexponentially with a time constant in the order of a microsecond (1.17 μs for **5** and 6.97 μs for **6**), yielding intrinsic quantum yields (Φ_{Ln} = 0.45% for **5** and 0.35% for **6**) lower than those for complexes **1** and **2**. It should be noted that, for the two series of complexes in solution, each Ln^{3+} ion is encapsulated by two asymmetric Schiff base ligands, which make it exposed to interactions with solvates (dmf or CH_3CN) molecules, which can result in partial luminescence quenching from C–H vibrational oscillators with relatively lower intrinsic quantum yields.[27] The addition of the heavy atom in the second series of complexes has no expected beneficial effect on the enhancement of NIR luminescence, which supports the hypothesis that the NIR sensitization occurs by energy transfer from the ^{1}LC but not the ^{3}LC excited state to the Ln^{3+} ion. It also suggests that the more effective vibronic quenching by the C–H vibrations results from the smaller energy gap between the lowest luminescent state and the highest nonluminescent state of the lanthanide

ions.[37] Although we do not have enough NIR luminescence information for the two Er^{3+} complexes (**3** and **7**), with their concentrations in dilute CH_3CN solutions adjusted to give the same absorbance at 355 nm, the relative emission intensity at 1440 nm for **7**, which has Br atoms, was about 1.5 times that of **3**, and this ratio is much higher in CD_3CN than CH_3CN (3.3:1).[19f,28]

Table 3. Crystal data and refinement for complexes **1** and **5**.

Compound	**1**	**5**
Empirical formula	$C_{72}H_{86}N_{12}Nd_2O_{27}Zn_2$	$C_{56}H_{58}Br_2N_{12}Nd_2O_{26}Zn_2$
Formula weight	1970.75	2054.00
Crystal system	triclinic	monoclinic
Space group	$P\bar{1}$	$P2_1/c$
a (Å)	12.9470(6)	12.034(2)
b (Å)	13.8620(7)	17.983(3)
c (Å)	13.9253(5)	16.910(3)
α (°)	101.007(4)	90
β (°)	109.947(4)	108.524(3)
γ (°)	111.971(5)	90
V (Å^3)	2027.97(16)	3469.9(10)
Z	1	2
ρ (gcm^{-3})	1.614	1.966
Crystal size (mm)	0.35× 0.28× 0.23	0.31× 0.25× 0.21
μ(Mo-K_α) (mm^{-1})	1.929	4.546
T (K)	293(2)	273(2)
Data/restraints/parameters	9964/0/ 520	7125/0/464
Quality-of-fit indicator	0.983	0.736
Final R indices	R_1 = 0.0579	R_1 = 0.0445
[$I>2\sigma(I)$]	wR_2 = 0.1211	wR_2 = 0.0867
R indices (all data)	R_1 = 0.0965	R_1 = 0.1275
	$wR2$ = 0.1310	wR_2 = 0.1001

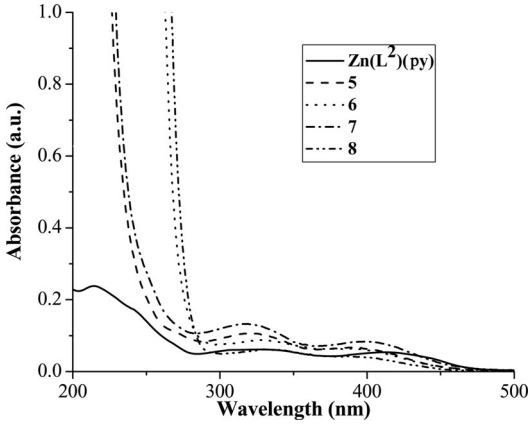

Figure 6. UV/Vis spectra of [Zn(HL^2)(py)] and complexes **5**–**8** in CH_3CN solution (1× 10^{-5} M) at room temperature.

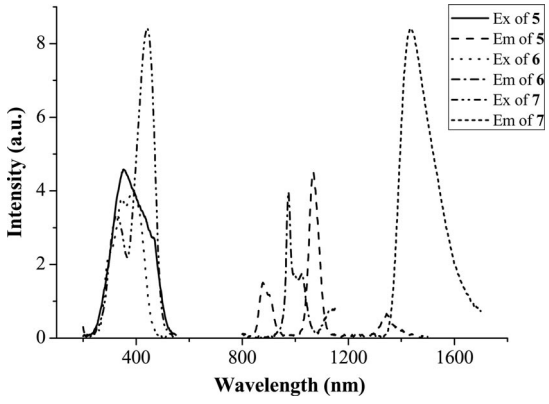

Figure 7. NIR emission and excitation spectra of complexes **5**–**7** in CH_3CN solution (1× 10^{-5} M) at room temperature.

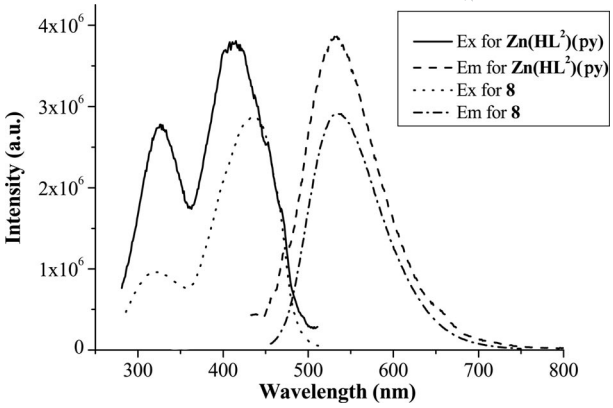

Figure 8. Visible emission and excitation spectra of [Zn(HL^2)(py)] and complex **8** in CH_3CN solution (1× 10^{-5} M) at room temperature.

Conclusions

Two series of cyclic tetranuclear complexes $[Zn_2(L^1)_2(py)_2Ln_2(NO_3)_4(dmf)_2]\cdot 3Et_2O$ (Ln = Nd, **1**; Yb, **2**; Er, **3**; and Gd, **4**) and $[Zn_2(L^2)_2Ln_2(NO_3)_4(dmf)_4]$ (Ln = Nd, **5**; Yb, **6**; Er, **7**; and Gd, **8**) were obtained from the reaction of the Zn-containing "complex ligand" [Zn(HL^1)(py)] and [Zn(HL^2)(py)] (py = pyridine) with $Ln(NO_3)_3\cdot 6H_2O$. Results of photophysical studies show that, with excitation at 200–550 nm, corresponding to the intraligand π→π* transitions of the Schiff base, strong and characteristic NIR luminescence of the Ln^{3+} ions with emissive lifetimes in the microsecond range were sensitized from the excited state (^{1}LC) of the ligand, whereas the ^{1}LC visible fluorescence is mostly quenched because of efficient intramolecular energy transfer from the ^{1}LC excited state to the Ln^{3+} ions. In addition, the occupation of pyridine groups in axial positions of the Zn^{2+} ions and the involvement of heavy atoms help to enhance the NIR luminescence to some extent. Further exclusion of vibronic deactivating solvent molecules from the inner coordination sphere of the complexes should be feasible through the use of additional ligands or more sterically demanding anions. Work in this direction is now under way.

Experimental Section

General: All chemicals were commercial products of reagent grade and were used without further purification. Elemental analyses were performed with a Perkin–Elmer 240C elemental analyzer. Infrared spectra were recorded with a Nicolet Nagna-IR 550 spectrophotometer in the region 4000–400 cm^{-1} by using KBr pellets. ^{1}H NMR spectra were recorded with a JEOL EX-270 spectrometer in $CDCl_3$ at room temp. ESI-MS was performed with a Finnigan LCQ^{DECA} XP HPLC-MS$_n$ mass spectrometer with a mass-to-

charge (m/z) range of 4000 with a standard electrospray ion source and CH_3CN as solvent. Electronic absorption spectra in the UV/Vis region were recorded with a Cary 300 UV spectrophotometer, steady-state visible fluorescence, PL excitation spectra with a Photon Technology International (PTI) Alphascan spectrofluorometer, and visible decay luminescence spectra with a pico-N_2 laser system (PTI Time Master). The quantum yield of the visible luminescence for each sample was determined by the relative comparison procedure with use of a reference of known quantum yield (quinine sulfate in dilute H_2SO_4 solution, $\Phi_{em} = 0.546$). NIR emission and excitation in solution were recorded with a PTI QM4 spectrofluorometer having a PTI QM4 Near-Infrared InGaAs detector. The X-ray powder diffraction pattern was recorded with a D/Max-IIIA diffractometer having graphite-monochromated Cu-K_α radiation (λ = 1.5418 Å).

Syntheses

[Zn(HL^1)(py)] or [Zn(HL^2)(py)]: To a stirred solution of 2,3-diaminophenol (1.3 g, 10 mmol) and *o*-vanillin (3.6 g, 20 mmol) or 5-bromo-3-methoxy-benzaldehyde (4.8 g, 20 mmol) in absolute EtOH (4 mL) were added $Zn(OAc)_2{\cdot}2H_2O$ (2.2 g, 10 mmol) and pyridine (2 mL). The reaction mixture was heated under reflux overnight. The resulting precipitate was filtered, washed with cold EtOH and $CHCl_3$, and dried under vacuum to give [Zn(HL^1)(py)] or [Zn(HL^2)(py)] as yellow solids in moderate yields.

For [Zn(HL^1)(py)]: Yield: 3.1 g (58%). $C_{27}H_{23}N_3O_5Zn$ (534.88): calcd. C 60.63, H 4.33, N 7.86; found C 60.48, H 4.56, N 7.67. IR (KBr): $\tilde{\nu}$ = 3391 (b), 1609 (s), 1534 (m), 1463 (vs), 1352 (w), 1321 (w), 1235 (s), 1201 (m), 1118 (m), 974 (m), 870 (w), 840 (w), 725 (m), 695 (w), 565 (w), 515 (w), 432 (w) cm^{-1}. ^{1}H NMR (270 MHz, $CDCl_3$): δ = 11.14 (s, 1 H, O*H*), 9.93 (s, 1 H, N=C*H*), 9.45 (s, 1 H, N=C*H*), 8.86 (d, J = 1.7 Hz, 1 H, py*H*), 8.65 (d, J = 1.9 Hz, 1 H, py*H*), 8.46 (m, 1 H, py*H*), 8.02 (m, 1 H, py*H*), 7.70 (m, 1 H, py*H*), 7.41 (m, 1 H, Ar*H*), 7.31 (d, J = 5.3 Hz, 1 H, Ar*H*), 7.27 (m, 1 H, Ar*H*), 7.19 (d, J = 4.6 Hz, 1 H, Ar*H*), 7.12 (d, J = 4.1 Hz, 1 H, Ar*H*), 6.98 (d, J = 4.6 Hz, 1 H, Ar*H*), 6.81 (d, J = 5.4 Hz, 1 H, Ar*H*), 6.74 (m, 1 H, Ar*H*), 6.59 (d, J = 4.5 Hz, 1 H, Ar*H*), 3.75 (s, 3 H, OC*H*$_3$), 3.63 (s, 3 H, OC*H*$_3$) ppm.

For [Zn(HL^2)(py)]: Yield: 4.2 g (61%). $C_{27}H_{21}Br_2N_3O_5Zn$ (692.67): calcd. C 46.82, H 3.06, N 6.07; found C 46.73, H 3.32, N 6.01. IR (KBr): $\tilde{\nu}$ = 3442 (b), 1599 (s), 1534 (s), 1466 (vs), 1382 (w), 1279 (s), 1236 (m), 1210 (m), 1094 (w), 1025 (m), 965 (m), 845 (w), 814 (m), 785 (m), 752 (m), 698 (w), 522 (m), 432 (w) cm^{-1}. ^{1}H NMR (270 MHz, $CDCl_3$): δ = 11.04 (s, 1 H, O*H*), 9.86 (s, 1 H, N=C*H*), 9.31 (s, 1 H, N=C*H*), 8.72 (d, J = 1.9 Hz, 1 H, py*H*), 8.53 (d, J = 2.4 Hz, 1 H, py*H*), 8.20 (m, 1 H, py*H*), 8.11 (m, 1 H, py*H*), 7.52 (m, 1 H, py*H*), 7.33–7.31 (m, 3 H, Ar*H*), 7.21 (s, 1 H, Ar*H*), 7.18–7.06 (m, 2 H, Ar*H*), 6.99 (s, 1 H, Ar*H*), 3.93 (s, 3 H, OC*H*$_3$), 3.72 (s, 3 H, OC*H*$_3$) ppm.

[Zn$_2$(L^1)$_2$(py)$_2$Ln$_2$(NO$_3$)$_4$(dmf)$_2$]·3Et$_2$O (Ln = Nd, 1; Yb, 2; Er, 3; and Gd, 4): To a stirred suspension of [Zn(HL^1)(py)] (0.107 g, 0.20 mmol) in absolute EtOH (3 mL) was added a solution of $Ln(NO_3)_3{\cdot}6H_2O$ (0.20 mmol, Ln = Nd, 0.088 g; Ln = Yb, 0.091 g; Ln = Er, 0.090 g; Ln = Gd, 0.090 g) and triethylamine (30 μL) in anhydrous dmf (3 mL), and the reaction mixture was heated under reflux (3 h) to give a clear yellow solution, which was then cooled to room temp. and filtered. Diethyl ether was allowed to diffuse slowly into the filtrate at room temp. Microcrystals of [Zn$_2$(L^1)$_2$(py)$_2$Ln$_2$(NO$_3$)$_4$(dmf)$_2$]·3Et$_2$O (Ln = Nd, **1**; Yb, **2**; Er, **3**; Gd, **4**) were obtained in three weeks.

For 1: Red crystals; yield: 0.093 g (47%). $C_{72}H_{86}N_{12}Nd_2O_{27}Zn_2$ (1970.75): calcd. C 43.88, H 4.40, N 8.53; found C 43.67, H 4.62, N 8.27. IR (KBr): $\tilde{\nu}$ = 2932 (w), 1653 (s), 1598 (s), 1543 (m), 1465 (vs), 1380 (m), 1296 (s), 1212 (m), 1074 (m), 1021 (m), 960 (m), 846 (w), 786 (w), 735 (m), 670 (w), 633 (w), 517 (m), 418 (w) cm^{-1}.

For 2: Yellow crystals; yield: 0.103 g (51%). $C_{72}H_{86}N_{12}O_{27}Yb_2Zn_2$ (2028.38): calcd. C 42.63, H 4.27, N 8.29; found C 42.42, H 4.51, N 8.13. IR (KBr): $\tilde{\nu}$ = 2938 (w), 1651 (s), 1608 (s), 1550 (m), 1468 (vs), 1382 (m), 1295 (s), 1209 (m), 1071 (m), 1026 (m), 958 (m), 850 (w), 788 (w), 745 (m), 701 (w), 571 (w), 519 (m), 444 (w) cm^{-1}.

For 3: Yellow crystals; yield: 0.083 g (41%). $C_{72}H_{86}Er_2N_{12}O_{27}Zn_2$ (2016.82): calcd. C 42.88, H 4.30, N 8.33; found C 42.91, H 4.16, N 8.52. IR (KBr): $\tilde{\nu}$ = 2935 (w), 1657 (s), 1608 (s), 1548 (m), 1509 (m), 1468 (vs), 1390 (m), 1285 (s), 1232 (m), 1205 (m), 1072 (m), 1022 (m), 960 (m), 849 (w), 785 (w), 740 (m), 700 (w), 630 (w), 572 (w), 518 (m), 445 (w) cm^{-1}.

For 4: Red crystals; yield: 0.104 g (52%). $C_{72}H_{86}Gd_2N_{12}O_{27}Zn_2$ (1996.80): calcd. C 43.31, H 4.34, N 8.42; found C 43.17, H 4.53, N 8.62. IR (KBr): $\tilde{\nu}$ = 2934 (w), 1651 (m), 1607 (s), 1546 (m), 1501 (m), 1467 (vs), 1391 (m), 1289 (s), 1231 (m), 1204 (m), 1072 (m), 1022 (m), 960 (m), 847 (w), 787 (w), 740 (m), 698 (w), 572 (w), 514 (m), 445 (w) cm^{-1}.

[Zn$_2$(L^2)$_2$Ln$_2$(NO$_3$)$_4$(dmf)$_4$] (Ln = Nd, 5; Yb, 6; Er, 7; and Gd, 8): To a stirred suspension of [Zn(HL^2)(py)] (0.114 g, 0.20 mmol) in absolute EtOH (3 mL) was added a solution of $Ln(NO_3)_3{\cdot}6H_2O$ (0.20 mmol, Ln = Nd, 0.088 g; Ln = Yb, 0.091 g; Ln = Er, 0.090 g; Ln = Gd, 0.090 g) in anhydrous dmf (3 mL), and the reaction mixture was refluxed for about 3 h to give a clear yellow solution, which was then cooled to room temp. and filtered. Diethyl ether was allowed to diffuse slowly into the filtrate at room temp. Microcrystals of [Zn$_2$(L^2)$_2$Ln$_2$(NO$_3$)$_4$(dmf)$_4$] (Ln = Nd, **5**: Yb, **6**; Er, **7**; and Gd, **8**) were obtained in about three weeks.

For 5: Red crystals; yield: 0.117 g, 57%. $C_{56}H_{58}Br_4N_{12}Nd_2O_{26}Zn_2$ (2054.00): calcd. C 32.75, H 2.85, N 8.18; found C 32.58, H 2.96, N 8.13. IR (KBr): $\tilde{\nu}$ = 2933 (w), 1654 (s), 1594 (m), 1537 (m), 1464 (vs), 1381 (m), 1295 (s), 1226 (m), 1094 (m), 1027 (m), 963 (m), 786 (m), 734 (w), 694 (w), 606 (w), 570 (w), 520 (w) cm^{-1}.

For 6: Yellow crystals; yield: 0.098 g, 46%. $C_{56}H_{58}Br_4N_{12}O_{26}Yb_2Zn_2$ (2111.60): calcd. C 31.85, H 2.77, N 7.96; found C 31.78, H 2.86, N 7.83. IR (KBr): $\tilde{\nu}$ = 2922 (w), 1658 (s), 1599 (s), 1534 (s), 1466 (vs), 1382 (m), 1279 (s), 1236 (m), 1210 (m), 1094 (w), 1025 (m), 965 (m), 845 (w), 814 (m), 785 (m), 752 (w), 698 (m), 522 (m) cm^{-1}.

For 7: Yellow crystals; yield: 0.100 g, 43%. $C_{56}H_{58}Br_4Er_2N_{12}O_{26}Zn_2$ (2100.04): calcd. C 32.03, H 2.78, N 8.00; found C 29.92, H 2.96, N 7.93. IR (KBr): $\tilde{\nu}$ = 2921 (w), 1658 (s), 1597 (s), 1535 (m), 1466 (vs), 1383 (s), 1281 (s), 1235 (m), 1210 (m), 1093 (w), 1027 (m), 965 (m), 844 (w), 814 (m), 785 (m), 753 (m), 699 (m), 612 (w), 570 (w), 522 (m) cm^{-1}.

For 8: Red crystals; yield: 0.106 g, 51%. $C_{56}H_{58}Br_4Gd_2N_{12}O_{26}Zn_2$ (2080.02): calcd. C 32.34, H 2.81, N 8.08; found C 32.28, H 2.96, N 8.02. IR (KBr): $\tilde{\nu}$ = 2932 (w), 1653 (s), 1596 (s), 1537 (m), 1465 (vs), 1380 (m), 1298 (s), 1230 (m), 1097 (m), 1026 (m), 964 (m), 786 (m), 696 (m), 607 (m), 571 (m), 521 (w) cm^{-1}.

Crystal Structure Determination: Single crystals of **1** and **5** of suitable dimensions were mounted onto thin glass fibers. All the intensity data were collected with a Bruker SMART CCD diffractometer (Mo-K_α radiation, λ = 0.71073 Å) in Φ and ω scan modes. Structures were solved by direct methods followed by difference Fourier syntheses, and then refined by full-matrix least-squares techniques against F^2 with SHELXTL.[38] All other non-hydrogen atoms were refined with anisotropic thermal parameters. Absorption correc-

tions were applied by using SADABS.[39] All hydrogen atoms were placed in calculated positions and refined isotropically by using a riding model. Crystallographic data and refinement parameters for the complexes are presented in Table 3. Relevant atomic distances and bond angles are collected in Table 2. CCDC-721334 (for **1**) and -720708 (for **5**) contain the supplementary crystallographic data for this paper. These data can be obtained free of charge from The Cambridge Crystallographic Data Centre via www.ccdc.cam.ac.uk/data_request/cif.

Acknowledgments

This work is funded by the National Natural Science Foundation (20871098), the Provincial Key Item of Shaanxi, the Provincial Natural Foundation of Shaanxi (2007B03), Education Committee Foundation of Shaanxi Province (07JK391), Graduate Cross-discipline Funds (07YJC11 and 09YJC23), and Graduate Innovation and Creativity Funds (08YZZ48) of Northwest University, Hong Kong Research Grants Council in P. R. China (HKBU 202407), the Welch Foundation (Grant F 816), the Texas Higher Education Coordinating Board (ARP 003658-0010-2006) and the Petroleum Research Fund, administered by the American Chemical Society (47014-AC5).

[1] a) R. Weissleder, N. Ntziachristos, *Nat. Med.* **2003**, *9*, 123–128; b) S. Kim, Y. T. Lim, E. G. Soltesz, A. M. De Grand, J. Lee, A. Nakayama, J. A. Parker, T. Mihaljevic, R. G. Laurence, D. M. Dor, L. H. Cohn, M. G. Bawendi, J. V. Frangioni, *Nat. Biotechnol.* **2004**, *22*, 93–97; c) S. Comby, J. C. G. Bünzli in *Handbook on the Physics and Chemistry of Rare Earths, Vol. 37*, (Eds.: K. A. Gschneider Jr., J. C. G. Bünzli, V. K. Pecharsky), Elsevier, Amsterdam, **2007**, p. 217–410.

[2] L. Winkless, R. H. C. Tan, Y. Zheng, M. Motevalli, P. B. Wyatt, W. P. Gillin, *Appl. Phys. Lett.* **2006**, *89*, 11115–11116.

[3] a) A. O'Riordan, R. Van Deun, E. Mairiaux, S. Moynihan, P. Fias, P. Nockemann, K. Binnemans, G. Redmond, *Thin Solid Films* **2008**, *516*, 5098–5102; b) S. V. Eliseevaa, J.-C. G. Bunzli, *Chem. Soc. Rev.* **2010**, *39*, 189–227.

[4] J. C. G. Bünzli, C. Piguet, *Chem. Soc. Rev.* **2005**, *34*, 1048–1077.

[5] a) S. Faulkner, B. P. Burton-Pye, T. Khan, L. R. Martin, S. D. Wray, P. J. Skabara, *Chem. Commun.* **2002**, 1668–1669; b) H.-S. He, X.-J. Zhu, A.-X. Hou, J.-P. Guo, W.-K. Wong, W.-Y. Wong, K.-F. Li, K.-W. Cheah, *Dalton Trans.* **2004**, 4064–4073; c) S. J. A. Pope, B. P. Burton-Pye, R. Berridge, T. Khan, P. J. Skabara, S. Faulkner, *Dalton Trans.* **2006**, 2907–2912.

[6] a) H.-S. Wang, G.-D. Qian, M.-Q. Wang, J.-H. Zhang, Y.-S. Luo, *J. Phys. Chem. B* **2004**, *108*, 8084–8088; b) D. Imbert, S. Comby, A.-S. Chauvin, J. C. G. Bünzli, *Chem. Commun.* **2005**, 1432–1434; c) M.-K. Nah, S.-G. Rho, H. K. Kim, J.-G. Kang, *J. Phys. Chem. A* **2007**, *111*, 11437–11443; d) M. Giraud, E. S. Andreiadis, A. S. Fisyuk, R. Demadrille, J. Pécaut, D. Imbert, M. Mazzanti, *Inorg. Chem.* **2008**, *47*, 3952–3954; e) A. P. S. Samuel, E. G. Moore, M. Melchior, J.-D. Xu, K. N. Raymond, *Inorg. Chem.* **2008**, *47*, 7535–7544.

[7] M. D. Ward, *Coord. Chem. Rev.* **2007**, *251*, 1663–1677.

[8] a) D. Imbert, M. Cantnuel, J. C. G. Bünzli, G. Bernardinelli, C. Piguet, *J. Am. Chem. Soc.* **2003**, *125*, 15698–15699; b) S. Torelli, D. Imbert, M. Cantnuel, G. Bernardinelli, S. Delahaye, A. Hauser, J. C. G. Bünzli, C. Piguet, *Chem. Eur. J.* **2005**, *11*, 3228–3242.

[9] W.-K. Wong, A.-X. Hou, J.-P. Guo, H.-S. He, L.-L. Zhang, W.-Y. Wong, K.-F. Li, K.-W. Chean, F. Xue, T. C. W. Mak, *J. Chem. Soc., Dalton Trans.* **2001**, 3092–3098.

[10] S. Akine, T. Taniguchi, T. Nabeshima, *Angew. Chem. Int. Ed.* **2002**, *41*, 4670–4673.

[11] a) S. I. Klink, H. Keizer, F. C. J. M. van Veggel, *Angew. Chem. Int. Ed.* **2000**, *39*, 4319–4321; b) D. Guo, C.-Y. Duan, F. Lu, Y. Hasegawa, Q.-J. Meng, S. Yanagida, *Chem. Commun.* **2004**, 1486–1487; c) C. Giansante, P. Ceroni, V. Balzani, F. Vögtle, *Angew. Chem. Int. Ed.* **2008**, *47*, 5422–5423.

[12] A. Beeby, R. S. Dickins, S. FitzGerald, L. J. Govenlock, C. L. Maupin, D. Parker, J. P. Riehl, G. Siligardi, J. A. G. Williams, *Chem. Commun.* **2000**, 1183–1184.

[13] a) P. B. Glover, P. R. Ashton, L. J. Childs, A. Rodger, M. Kercher, R. M. Williams, L. de Cola, Z. Pikramenou, *J. Am. Chem. Soc.* **2003**, *125*, 9918–9919; b) H.-B. Xu, L.-X. Shi, E. Ma, L.-Y. Zhang, Q.-H. Wei, Z.-N. Chen, *Chem. Commun.* **2006**, 1601–1603; c) X.-L. Li, F.-R. Dai, L.-Y. Zhang, Y.-M. Zhu, Q. Peng, Z.-N. Chen, *Organometallics* **2007**, *26*, 4483–4490; d) H.-B. Xu, L.-Y. Zhang, Z.-H. Chen, L.-X. Shi, Z.-N. Chen, *Dalton Trans.* **2008**, 4664–4670; e) J. Ni, L.-Y. Zhang, Z.-N. Chen, *J. Organomet. Chem.* **2009**, *694*, 339–345.

[14] a) M. Mehlstäubl, G. S. Kottas, S. Colella, L. de Cola, *Dalton Trans.* **2008**, 2385–2388; b) F.-F. Chen, Z.-Q. Bian, B. Lou, E. Ma, Z.-W. Liu, D. B. Nie, Z.-Q. Chen, J. Bian, Z.-N. Chen, C.-H. Huang, *Dalton Trans.* **2008**, 5577–5583.

[15] H.-B. Xu, L.-Y. Zhang, J. Ni, H.-Y. Chao, Z.-N. Chen, *Inorg. Chem.* **2008**, *47*, 10744–10752.

[16] B. Zhao, X.-Q. Zhao, Z. Chen, W. Shi, P. Cheng, S.-P. Yan, D.-Z. Liao, *CrystEngComm* **2008**, *10*, 1144–1146.

[17] Y.-X. Chi, S.-Y. Niu, Z.-J. Wang, J. Jin, *Eur. J. Inorg. Chem.* **2008**, 2336–2343.

[18] S. J. A. Pope, B. J. Coe, S. Faulkner, R. H. Laye, *Dalton Trans.* **2005**, 1482–1490.

[19] a) W.-K. Wong, H.-Z. Liang, W.-Y. Wong, Z.-W. Cai, K.-F. Li, K.-W. Cheah, *New J. Chem.* **2002**, *26*, 275–278; b) W.-K. Lo, W.-K. Wong, J.-P. Guo, W.-Y. Wong, K.-F. Li, K.-W. Cheah, *Inorg. Chim. Acta* **2004**, *357*, 4510–4521; c) W.-K. Lo, W.-K. Wong, W.-Y. Wong, J.-P. Guo, K.-T. Yeung, Y.-K. Cheng, X.-P. Yang, R. A. Jones, *Inorg. Chem.* **2006**, *45*, 9315–9325; d) X.-P. Yang, R. A. Jones, Q.-Y. Wu, M. M. Oye, W.-K. Lo, W.-K. Wong, A. L. Holmes, *Polyhedron* **2006**, *25*, 271–278; e) W.-Y. Bi, X.-Q. Lü, W.-L. Chai, J.-R. Song, W.-Y. Wong, W.-K. Wong, R. A. Jones, *J. Mol. Struct.* **2008**, *891*, 450–455; f) X.-P. Yang, R. A. Jones, M. M. Oye, A. L. Holmes, W.-K. Wong, *Cryst. Growth Des.* **2006**, *6*, 2122–2125.

[20] S. Mizukami, H. Houjou, K. Sugaya, E. Koyama, H. Tokuhisa, T. Sasaki, M. Kanesato, *Chem. Mater.* **2005**, *17*, 50–56.

[21] X.-P. Yang, R. A. Jones, V. Lynch, M. M. Oye, A. L. Holmes, *Dalton Trans.* **2005**, 849–851.

[22] W.-K. Wong, X.-P. Yang, R. A. Jones, J. H. Rivers, V. Lynch, W.-K. Lo, D. Xiao, M. M. Oye, A. L. Holmes, *Inorg. Chem.* **2006**, *45*, 4340–4345.

[23] W.-Y. Bi, T. Wei, X.-Q. Lü, Y.-N. Hui, J.-R. Song, S.-S. Zhao, W.-K. Wong, R. A. Jones, *New J. Chem.* **2009**, *33*, 2326–2334.

[24] X.-Q. Lü, W.-Y. Bi, W.-L. Chai, J.-R. Song, J.-X. Meng, W.-Y. Wong, W.-K. Wong, R. A. Jones, *New J. Chem.* **2008**, *32*, 127–131.

[25] a) X.-P. Yang, R. A. Jones, W.-K. Wong, M. M. Oye, A. L. Holmes, *Chem. Commun.* **2006**, 1836–1838; b) X.-Q. Lü, W.-Y. Bi, W.-L. Chai, J.-R. Song, J.-X. Meng, W.-Y. Wong, W.-K. Wong, X.-P. Yang, R. A. Jones, *Polyhedron* **2009**, *28*, 27–32.

[26] a) T. Kido, Y. Ikuta, Y. Sunatsuki, Y. Ogawa, N. Matsumoto, *Inorg. Chem.* **2003**, *42*, 398–408; b) S. Osa, T. Kido, N. Matsumoto, N. Re, A. Pochaba, J. Mrozinski, *J. Am. Chem. Soc.* **2004**, *126*, 420–421; c) J.-P. Costes, M. Auchel, F. Dahan, V. Peyrou, S. Shova, W. Wernsdorfer, *Inorg. Chem.* **2006**, *45*, 1924–1934; d) J.-P. Costes, S. Shova, W. Wernsdorfer, *Dalton Trans.* **2008**, 1843–1849.

[27] F. Quochi, R. Orru, F. Cordella, A. Mura, G. Bongiovanni, F. Artizzu, P. Deplanto, M. L. Mercurri, L. Pilla, A. Serpe, *J. Appl. Phys.* **2006**, *99*, 53520–53524.

[28] W.-Y. Bi, X.-Q. Lü, W.-L. Chai, J.-R. Song, W.-K. Wong, X.-P. Yang, R. A. Jones, *Z. Anorg. Allg. Chem.* **2008**, *634*, 1795–1800.

[29] M. Albrecht, O. Osetska, J. Klankermayer, R. Fröhlich, F. Gumy, J. C. G. Bünzli, *Chem. Commun.* **2007**, 1834–1836.

[30] M. J. Weber, *Phys. Rev.* **1968**, *171*, 283–291.
[31] J. Zhang, S. Petoud, *Chem. Eur. J.* **2008**, *14*, 1264–1272.
[32] J. C. G. Bünzli, S. Comby, A. S. Chauvin, C. D. B. Vandevyver, *J. Rare Earths* **2007**, *25*, 257–274.
[33] W. T. Carnall, P. R. Fields, K. Rajnak, *J. Chem. Phys.* **1968**, *69*, 4443–4446.
[34] G. Stein, E. Würzberg, *J. Chem. Phys.* **1975**, *62*, 208–213.
[35] D. L. Dexter, *J. Chem. Phys.* **1953**, *21*, 836–850.
[36] R. F. Ziessel, G. Ulrich, L. Charbonniere, D. Imbert, R. Scopelliti, J. C. G. Bünzli, *Chem. Eur. J.* **2006**, *12*, 5060–5067.
[37] S. I. Klink, L. Grave, D. M. Reinhoudt, F. C. J. M. van Veggel, M. H. V. Werts, F. A. J. Geurts, J. W. Hofstraat, *J. Phys. Chem. A* **2000**, *104*, 5457–5468.
[38] G. M. Sheldrick, *SHELXS-97: Program for Crystal Structure Refinement*, University of Göttingen, Göttingen, Germany, **1997**.
[39] G. M. Sheldrick, *SADABS*, University of Göttingen, Göttingen, Germany, **1996**.

Received: January 30, 2010
Published Online: May 21, 2010

